a

ingegneria sismica

International Journal of Earthquake Engineering

Anno XLIII - Num. 2 - 2026

Adaptability Study of Polyurethane Sealing Systems for Xinjiang Oilfields

Qianbing Lin[1], *Shiyu Wang*[2] *and Lianghui Guo*[1,*]

[1] School of Engineering, China University of Petroleum (Beijing), Karamay 834000 Xinjiang, China

[2] Xinjiang Key Laboratory of Safe Transportation of Multi-Medium Pipelines, Urumqi 830011, Xinjiang, China

SUMMARY: *Water breakthrough problems occur frequently during water injection in the mid-to-late stages of developing low-permeability reservoirs in Xinjiang, resulting in a sharp rise in water cut and reduced oil displacement efficiency. Development of a high-quality, injection-mouldable and sealing-performance-excellent, break-resistant system is required. Optimize the formulation of polyurethane resin in this study and examine how different temperatures, mineralisation, etc., affect the rheological properties and compressive strength of the system as well as its sealing performance. Based on the above results, the best curing composition is 40% polyurethane resin and 2% curing agent, at 80 ° C for 1 hour; this achieved a crack-free effect. High Mineralisation Reduced the Curing Period. Increase the proportion of curing agent and reduce deformation. Sealing performance tests showed that the 40%+2% polyurethane system had a maximum sealing rate of 96% and a breakthrough pressure gradient of 4.2 MPa·m⁻¹. Therefore, a new route will be developed to address water infiltration in the low-permeability reservoirs of Xinjiang.*

KEYWORDS: *Polyurethane; Low-permeability reservoir; Plugging and flow*

1 Introduction

Low-permeability reservoirs in Xinjiang are a typical example of areas for exploiting China's untapped oil and gas resources and have large oil and gas reserves [1, 2]. Because low-permeability reservoirs have little internal energy, the production efficiency of field development is generally relatively low in the middle and later stages. Application of pressure-driven water injection technology increases formation energy by high-pressure water injection, creates a network of microfractures to reduce oil-water flow resistance, and exploits the differences in oil-water two-phase flow to drive residual oil [3, 4] for a substantial improvement in recovery efficiency of low-permeability reservoirs. However, due to the reservoir conditions of a low-permeability reservoir—that is to say, high heterogeneity and dense natural fractures—the injected water is likely to flow rapidly along the main paths in the formation under pressure-driven injection [5-7]. As a result, there will be an increase in the well water cut and a substantial reduction in single-well production, leading to a water flooding problem. As of the end of 2024, the loss due to this reason in the Xinjiang Oilfield had exceeded 1 billion yuan. The time to water cut after pressure flooding for most wells was less than three months, and the proportion of ineffective injected water reached 35%; thus,

*guolh@cupk.edu.cn

https://doi.org/10.65102/is2026958

Published: 30 April, 2026

significant improvements in the economic efficiency of the Xinjiang Oilfield could not be achieved.

The current mainstream plugging technologies have serious deficiencies in the application to low-permeability reservoirs in Xinjiang: Among cement-based plugging agents, water-based types have large particle sizes and can only seal high-permeability formations; although ultrafine cement is suitable for low-permeability formations due to its small particle size, its rapid hydration rate, short initial setting time, and poor safety limit its field application [8, 9]; particle-based plugging agents are based on physical blockage, but their large particle size leads to issues such as poor suspension stability, low strength, poor performance, and a short effective period during water blocking operations in oilfields [10]. Gels are not stable at high temperatures and in the presence of high salinity; moreover, the gelation process cannot be effectively controlled, thus they are unsuitable for the requirements of low-permeability reservoirs in Xinjiang [11-13].

Due to their good mechanical properties, salt resistance and stable cross-linked structure, polyurethane materials are suitable for use in wellbore plugging [14-16]. Therefore, this study has optimised the formulation of a polyurethane plugging slurry for low-permeability reservoirs in Xinjiang and evaluated its rheological properties, compressive strength and plugging efficiency to provide technical support for controlling water ingress in low-permeability reservoirs in Xinjiang.

2 Experimental Section

2.1 Laboratory reagents

Polyurethane resin solution, 35% solids content, model YC-312, from Anhui Yuanchen New Materials Co., Ltd. Polyurethane curing agent, 100% solids content, model YC-8100, supplied by Anhui Yuanchen New Materials Co., Ltd.

As shown in the references [17-20], the formula for the simulated formation water at the Second Oil Production Plant of a certain oilfield in Xinjiang is as follows:

Table 1: Formulation for 30,000 TDS Formation Water

Ingredients	content (mg/L)
NaCl	7568.86
$NaHCO_3$	7087.6
$CaCl_2$	23.5
$MgCl_2$	21.4
Na_2SO_4	253.6

2.2 Laboratory equipment

Formation water, beakers, glass rods, droppers, stirrers, electronic balances, glass vials (30 mL), volumetric flasks (1000 mL), drying ovens, water baths, vacuum drying ovens, NDJ-8S viscometers, compressive strength testers and plug integrity testers.

2.3 Structural Characterization

Take a polyurethane resin solution as the basis and add the relevant curing agent. Prepare a 20-ml solution in a 30-ml glass vial using simulated formation water at a particular ratio. Mix

well with a glass stirring rod, close the vial, and then place it in an oven at 80 °C. Watch for Gelation every 30 minutes.

2.4 Structural Characterization

FTIR Characterization:

Prepare test samples in the KBr pellet method for Fourier transform infrared (FTIR) analysis. Dry the dried samples of the polyurethane sealant in a vacuum oven at 120°C for 1 hour, grind them into a powder, and uniformly disperse the powder on a KBr pellet. Measurement range: 400 cm^{-1} - 4000 cm^{-1}, 32 scans.

Scanning Electron Microscopy (SEM) analysis.

Send the prepared polyurethane sealant samples to Scientific Compass for scanning electron microscopy analysis.

2.5 Rheological properties

NDJ-8S viscometer and GB/T 22235-2008 were used for viscosity measurements. A prepared sealant system was put in a constant-temperature water bath, and then at different temperatures and shear rates, its viscosity was determined.

2.6 Compressive strength

Cut a 1-cm radius and 2-cm thick block from the cured sealant, place it in a compression testing machine to measure its strength, and note the value at which considerable deformation occurs; this is considered its compressive strength.

2.7 Sealing Performance

As shown in Figure 1, a displacement device was employed to investigate the plugging effect; sand was placed inside the sand-filled tube, compacted to simulate a reservoir, and then the dry weight of the sand was obtained. Simulated formation water was added to submerge the sand-filled tube, a vacuum was applied to determine the wet weight of the sand, and then the pore volume and porosity were calculated. With a displacement device, introduce formation water into the sand-filled tube at a rate of 1 mL/min. Reach a stable injection pressure, add over 2PV of formation water, and then record the pressure; at this point, calculate the initial permeability of the water phase. Inject the polyurethane sealing system into the sand-filled tube up to 1PV, then place it in an 85°C oven for ageing for 2 hours. Cool to room temperature, then carry out a water-phase backflush test by introducing simulated formation water in the opposite direction. Continue recording the change in pressure until the backflush volume reaches 10PV, then calculate the post-sealing water-phase permeability, water-phase sealing efficiency and breakthrough pressure. Feng Yachao, He Long and others [10] used the formula to calculate the sealing performance.

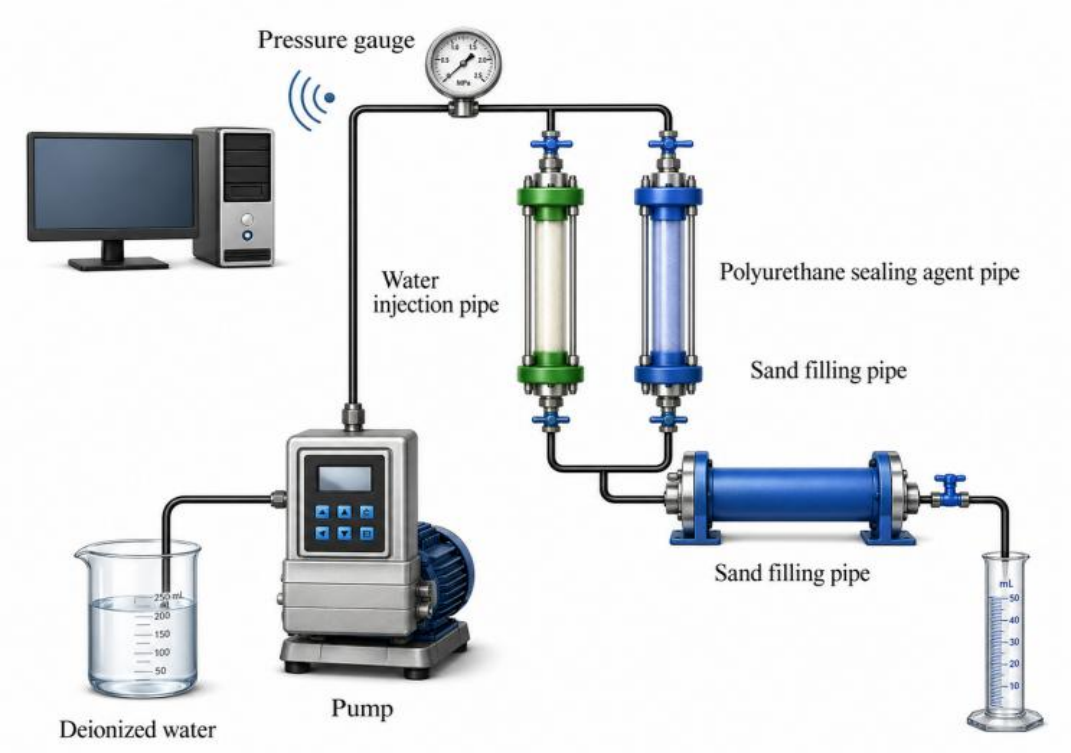

Figure 1: Plugging Verification Device

Penetration Rate

$$K = \frac{Q\mu L}{A\Delta P} \tag{1}$$

In Equation (1): K is the permeability, Q is the flow rate of the fluid pumped into the sand-filled pipe, μ is the viscosity of the fluid, L is the length of the sand-filled pipe, A is the cross-sectional area of the sand-filled pipe, and ΔP is the pressure difference.

Breaking through the Pressure Gradient

$$P_L = \frac{P_{max}}{L} \tag{2}$$

As shown in Equation (2), P_max is the breakthrough pressure after simulating the sealing of the core in a sand-filled tube; L is the length of the sand-filled tube; and P_L is the breakthrough pressure gradient.

Blockage Rate

$$F_S = \frac{K_1 - K_2}{K_1} \times 100\% \tag{3}$$

In Equation (3): F_S is the sealing efficiency; K_1 is the water injection permeability before the polyurethane sealing system seals the simulated core; and K_2 is the water injection permeability after the polyurethane sealing system seals the simulated core.

2.8 Salt tolerance

Prepare polyurethanes grouting system materials with simulated formation water of different degrees of mineralisation. At 80 °C in an oven, the sample was taken out every 30 minutes to

be observed, and at this time, the curing condition and curing time were recorded.

3 Results and Discussion

3.1 Formulation Optimization of Polyurethane Sealing Systems

To improve the formula of the polyurethane sealing system further, controlled-variable experiments were conducted to find the optimal concentration of resin and curing agent.

As shown in Table 2, at 80 °C, for a fixed amount of curing agent, the curing time first decreased and then increased with an increase in the concentration of polyurethane resin. At resin concentrations of 30% and 40%, the shortest curing times were achieved; the gel had completed within 1 hour. At a low resin concentration during the curing process, the system did not show any cracks after gelation. However, with an increase in resin concentration, the above phenomena of cracking and water separation (floating) were observed. The higher the amount of curing agent, the more pronounced the floating and water-separation phenomena. This is because, as the proportion of curing agent rises, strength and toughness also increase; therefore, there is a deviation in internal system pressure. The system with a 60% resin concentration had a much smaller number of cracks than the system with a 50% resin concentration, and there was no floating phenomenon. According to the experiment, the amount of curing agent did not change the time required for curing.

Table 2: Effect of Resin Concentration and Curing Agent Concentration on Gel Time in Polyurethane Sealant Systems

Curing agent concentration	Resin concentration				
	20%	30%	40%	50%	60%
0.5%	4.5h	1h	1h	1.5h	1.5h
1.5%	4.5h	1h	1h	1.5h	1.5h
2%	4.5h	1h	1h	1.5h	1.5h
2.5%	4.5h	1h	1h	1.5h	1.5h
3%	4.5h	1h	1h	1.5h	1.5h

Based on the above test results, the optimal formulations and ratios for the polyurethane resin sealing system have been determined as follows: 30% polyurethane resin + 2% curing agent, and 40% polyurethane resin + 2% curing agent. Curing for 1 hour at a temperature of 80 °C.

3.2 Structural Characterization

Fourier-transform infrared spectroscopy (FTIR) was employed to investigate changes in the structure of a curing agent and a polyurethane sealing system at different times after curing. The results are as follows: Figure 2.

A broad absorption band in the 3200-3500 cm^{-1} range due to the stretching vibration of the –OH group was observed before curing (a) and was reduced to a certain extent after curing (c). At the same time, a relatively sharp shoulder peak appeared at a lower wavenumber, corresponding to the N–H stretching vibration of the new –NHCOO– bond. After curing, a double-peaked structure appears at 1730 cm^{-1} and 1685 cm^{-1}, which are the characteristic absorption peaks of the C=O group in the –NHCOO– bond; thus, a typical urethane hard segment has been formed in the polyurethane structure. This is to show that it has cured. A stretching vibration peak of the C–O–C ether bond was found at 1135 cm^{-1}, and

it was determined that the polyether polyol soft segments had not been damaged during the reaction but had been fully preserved in the cross-linked network to form the flexible backbone of the material. In short, it can be seen from the above that the cured polyurethane sealing system has formed a typical cross-linked network structure, with polyether segments acting as the soft segments and urethane segments as the hard segments; it has good structural flexibility and cross-linking stability.

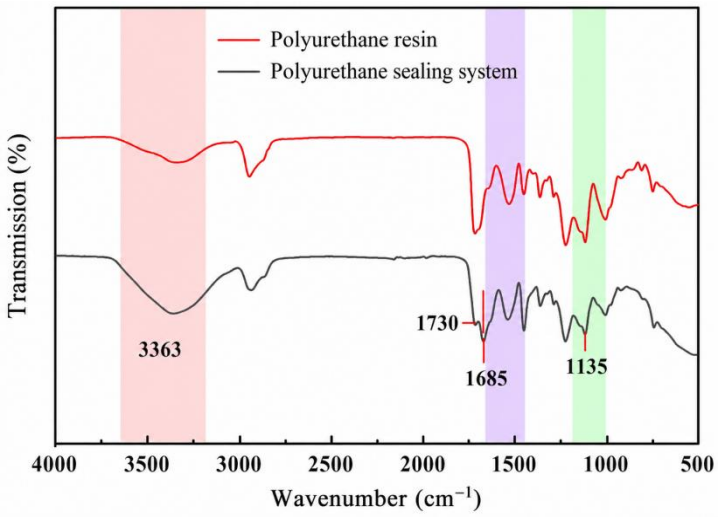

Figure 2: Infrared Spectra of Polyurethane Sealant System Before and After Curing

The structure at the microscale of a polyurethane resin-based sealing material was observed with a scanning electron microscope. Bright hard-segment microdomains were observed as the dispersed phase, uniformly embedded in a dark, continuous soft-segment matrix, and a typical "sea-island" two-phase separation structure was formed. The structure is due to strong intermolecular hydrogen bonding among the hard segments, and they are thus close-packed and highly ordered. These segments serve as the physical crosslinking sites and form a reinforcing network to increase the stiffness of the system. A continuous soft-segment matrix can absorb energy and is thus more flexible. As a result, the polyurethane sealing system has good strength and toughness, is relatively thermally stable, and is suitable for high-performance sealing applications at the macroscopic level.

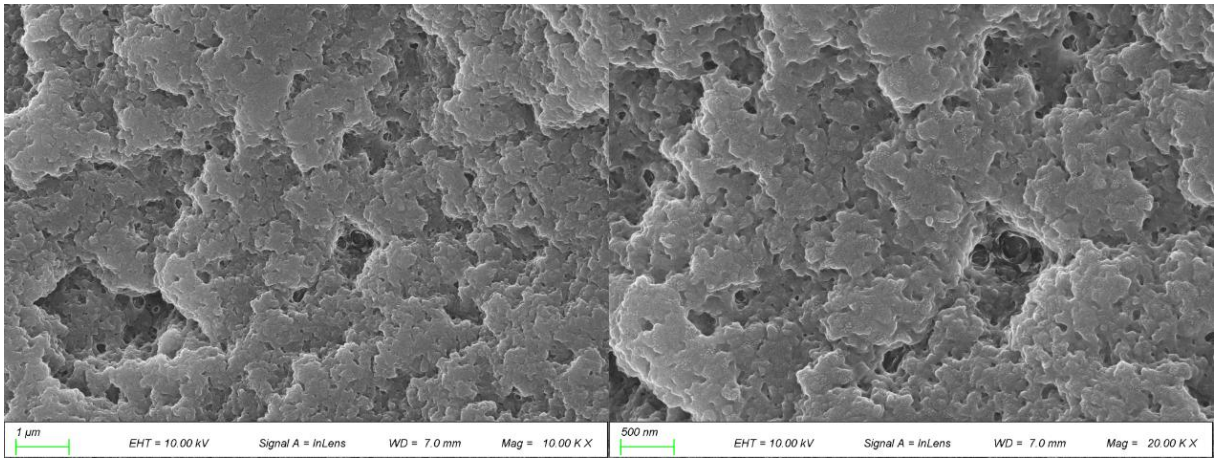

Figure 3: Scanning Electron Microscope Image of Polyurethane Sealing System

3.3 Curing properties

Another index of flowability for polyurethane grouting systems during injection that can be used is on-site applicability. An NDJ-8S viscometer will be used in this paper to find out how the viscosity of the system changes with different shear rates, and the corresponding results will be presented in Figure 4. As shown in the figure, at 75°C, with an increase in shear rate, the viscosity of both polyurethane systems at ratios of 30%+2% and 40%+2% decreased; that is to say, both exhibited shear-thinning behaviour typical of non-Newtonian fluids. The reason for the above phenomenon is that, under shear stress, the orientation and entanglement release of polyurethane molecular chains have decreased flow resistance.

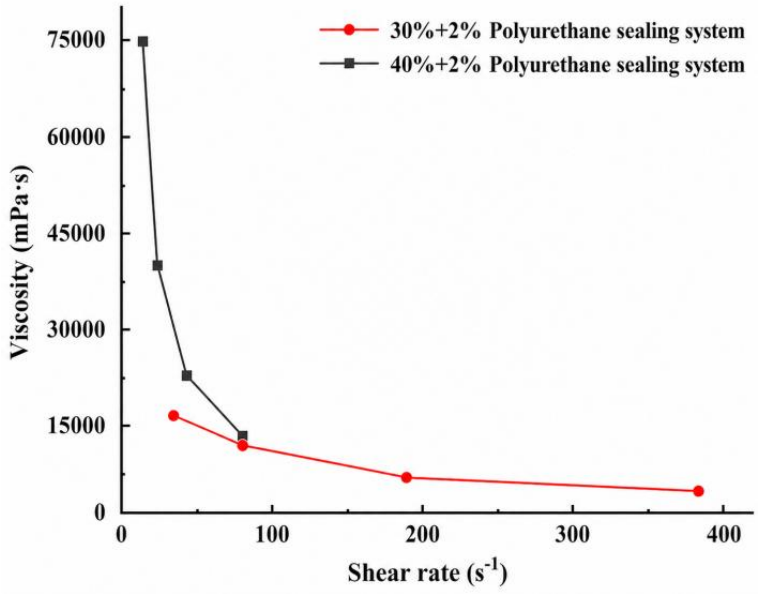

Figure 4: Effect of Shear Rate on Viscosity of the Polyurethane Encapsulation System

Another reason why the curing behaviour of polyurethane is affected is that of the salinity of the formation water. To simulate the actual operating environment of high-salinity formation water in Xinjiang oilfields, this paper systematically explores the effect of different salt concentrations (5-60 g/L) on the curing behaviour of two optimised formulations of polyurethane plugging systems, namely 30%+2% and 40%+2%. The results are as follows: Tables 3 and 4. According to the experiments, if the salinity was less than 10 g/L, the system could not gel; when the salinity reached 20 g/L or more, it could be fully cured in 1 hour, and under conditions of 60 g/L, the curing time was further reduced to 0.5 hours. This may be due to the "salt effect" of salt ions on the reactive groups of polyurethane; an increase in ionic strength can accelerate the reaction rate between isocyanate and active hydrogen, thus increasing the speed of formation for a cross-linked network. Additionally, the two formulations showed similar curing behaviour at different salt concentrations; therefore, it can be determined that this polyurethane system is highly salt-resistant and suitable for the complex formation water environment of the Xinjiang oilfield.

Table 3: Salt Concentration and Gel Formation of a 30%+2% Polyurethane Sealing System

Mineralization of groundwater(g/L)	5	10	20	30	40	60
Curing status	Not yet set	Not yet set	1h	1h	1h	0.5h

Table 4: Salt Concentration and Gel Formation of 40%+2% Polyurethane Sealing System

Mineralization of groundwater(g/L)	5	10	20	30	40	60
Curing status	Not yet set	Not yet set	1h	1h	1h	0.5h

Another Reason for changes in the speed and shape of a cured polyurethane is temperature. Systematically study the effect of temperature in the range of 50°C to 80°C on the curing behaviour of two optimised formulations, and present the results in Figure 5. With a rise in temperature, the required curing time of the system will decrease. For example, according to the 30%+2% system, the curing time at 50°C is 44 minutes, but when the temperature reaches 80°C, it has been reduced to only 5 minutes. High temperatures increase the reaction speed of the isocyanate group with the active group, and thus rapidly form a cross-linked network. It should be pointed out that at high temperatures, a porous bubble structure formed on the surface of the cured samples; this may be due to the production of local volatile byproducts caused by an exothermic reaction. Therefore, this structure will have a relatively low material density and strength. Comparing the two formulations, the 40% + 2% system had a faster curing speed and a more complete curing structure at all temperatures; thus, increasing the resin content can improve the high-temperature reactivity and structural stability of the system. Considering both the pumping time for field injection and the temperature conditions of the formation, the optimal curing temperature for the polyurethane plugging system is 80°C to meet the construction window and final performance requirements.

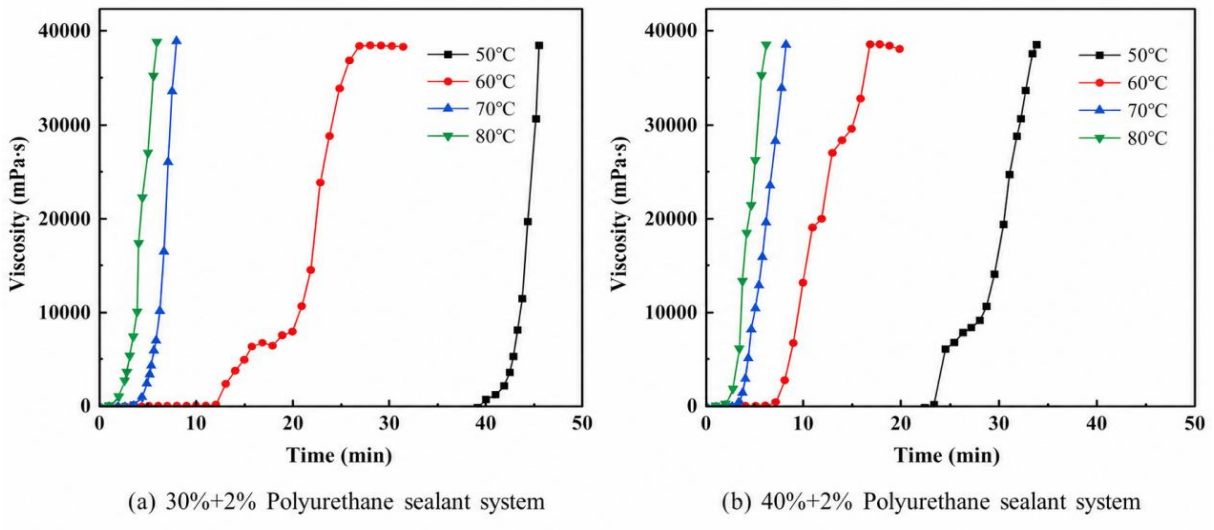

Figure 5: Curing Times of Polyurethane Sealant Systems at Different Temperatures (a) 30%+2% Polyurethane Sealant System (b) 40%+2% Polyurethane Sealant System

As shown in Figure 6, an increase in the ratio of the curing agent leads to a corresponding rise in stress and strain at the start, and the polyurethane grouting system is in an elastic deformation state at this time. As the load increases, the curve is no longer a straight line and has entered the plastic deformation region. An increase in the proportion of the curing agent will strengthen the bonding effect of the polyurethane grout system; thus, a high-curing-agent ratio system can bear more stress at a given strain. For example, in the 30%+2% polyurethane grouting system, at the same strain, the pressure value for the curve with a 6% curing agent concentration is significantly higher than that for the curve with a 2% curing agent concentration; a similar trend is also observed in the 40%+2% polyurethane grouting system. With an increase in the proportion of the curing agent, there is a reduced deformation of the

mixture under compression, and this change is consistent with the higher strength shown in the stress-strain curve.

As shown in Figures (a) and (b), at the same curing agent ratio, the 40%+2% polyurethane grouting system has a relatively better-retained shape after compression, and generally speaking, the 40%+2% system has superior strength to the 30%+2% system. Therefore, an increase in the proportion of resin can be used to improve the strength of a polyurethane grout.

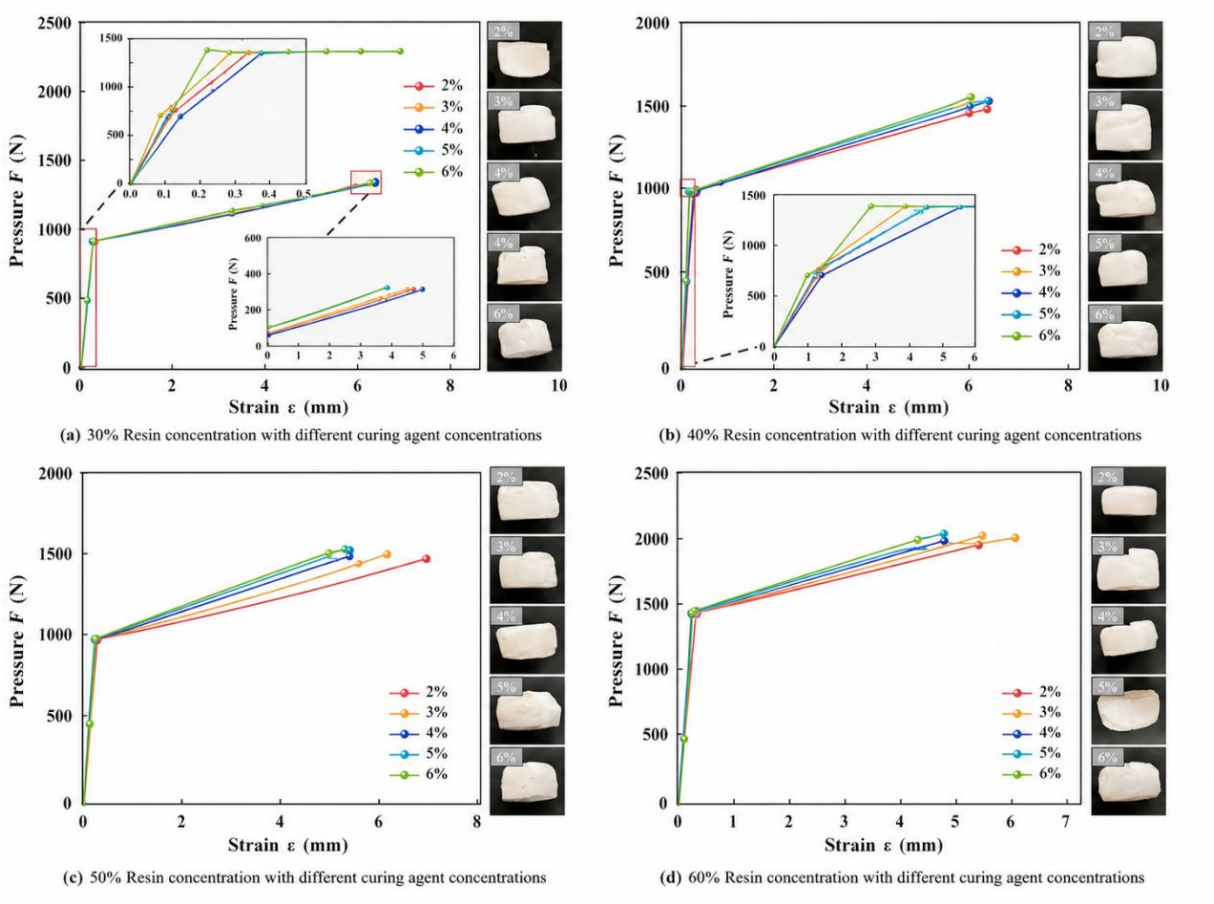

Figure 6: Strain-Stress Curves for Different Polyurethane Encapsulation Systems (a) 30% Resin Concentration with different curing agent concentrations (b) 40% Resin Concentration with different curing agent concentrations (c) 50% Resin Concentration with different curing agent concentrations (d) 60% Resin Concentration with different curing agent concentrations.

3.4 Shutdown Performance

A 30% + 2% polyurethane grout system has poorly cured in the core and formed sand clumps. On the other hand, a 40% + 2% polyurethane grouting system is used to cure inside the core, forms elongated strands, and can be recovered almost intact.

Figure 7: Sealing Performance Test of 40%+2% Sealing System

As shown in Figure 7, at a polyurethane content of 40%, the sealing efficiency reaches 96.00%; at a polyurethane content of 30%, it is a maximum of 92.30%. A High-resin compound can be used for Sealing. For all permeability values, the 40%+2% polyurethane sealing system generally has a higher sealing efficiency than the 30%+2% polyurethane sealing system. As shown in Figures (a) and (b), a higher resin content has been used for a more stable seal.

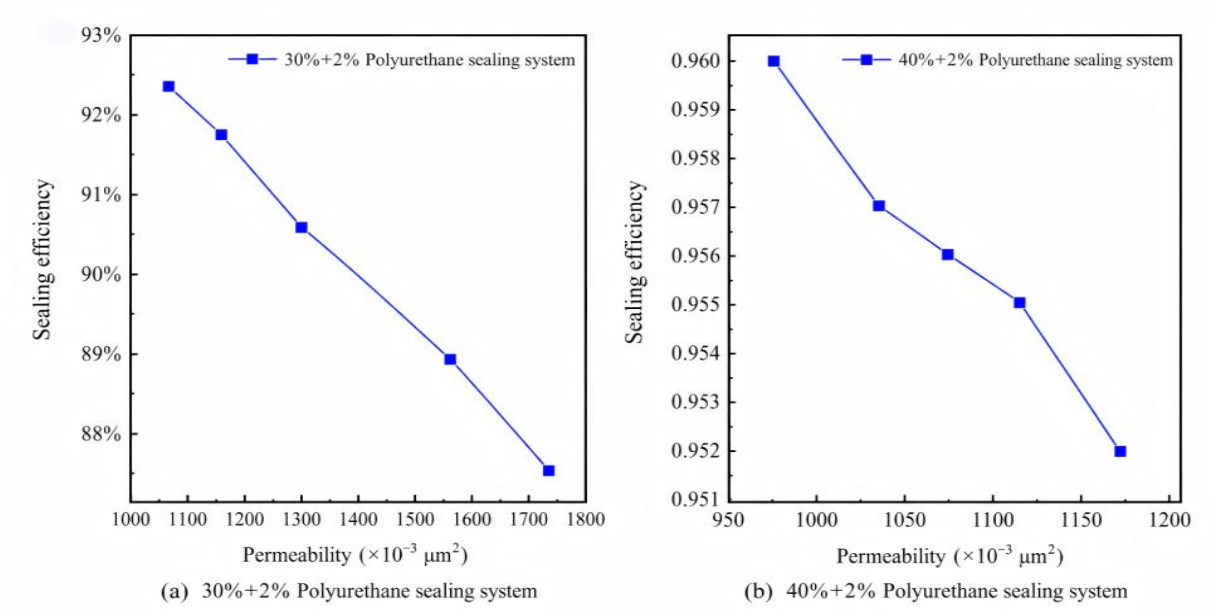

Figure 8: Permeability and Sealing Efficiency of Polyurethane Sealing Systems (a) 30%+2% Polyurethane Sealing System (b) 40%+2% Polyurethane Sealing System

As shown in Figure 8, at a polyurethane content of 40%, the maximum breakthrough pressure is 2.16 MPa·m^{-1}; when the polyurethane content is 30%, the sealing rate is 4.2 MPa·m^{-1}. A high-resin system can be more impermeable and thus more durable. Given the same permeability, the breakthrough pressure gradient of the 40%+2% polyurethane sealing system is generally higher than that of the 30%+2% polyurethane sealing system. A relatively high proportion of resin is needed to ensure good stability of the sealing performance; for example, the 40%+2% polyurethane sealing system showed a smaller drop in breakthrough pressure gradient with changes in permeability and was thus more stable under these conditions.

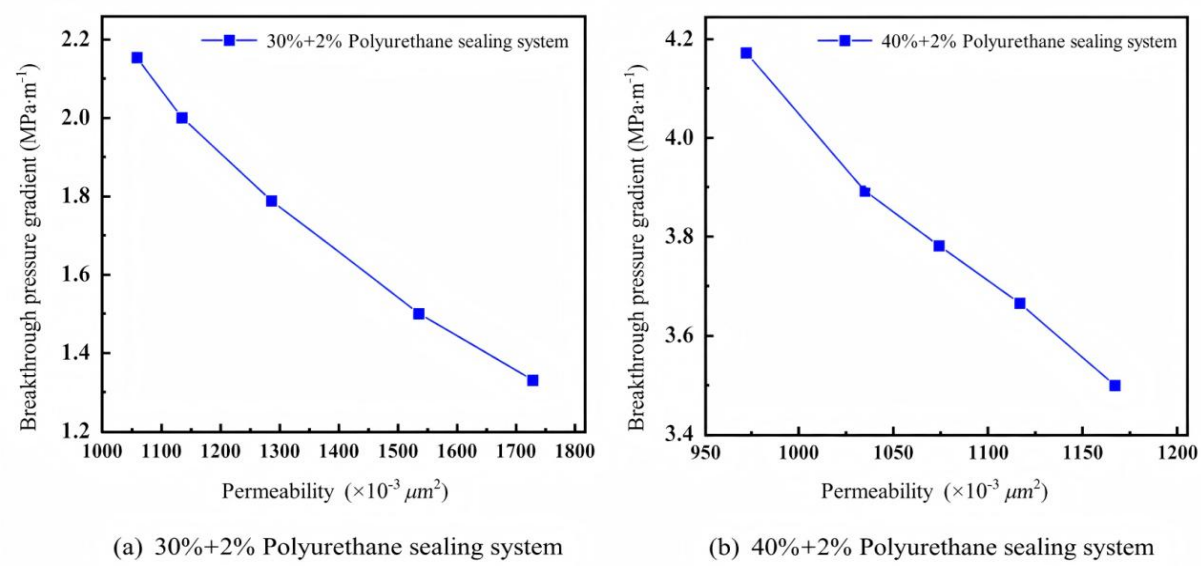

Figure 9: Permeability and Breakthrough Pressure Gradient of Polyurethane Sealing Systems (a) 30%+2% Polyurethane Sealing System (b) 40%+2% Polyurethane Sealing System

4 Summary

(1) The optimized polyurethane sealing system was 40% + 2% and 30% + 2%, with a curing temperature of 80°C and a curing time of 1 hour; no cracks were observed.

(2) Fourier transform infrared spectroscopy (FTIR) analysis confirms that the curing reaction of the polyurethane plugging system is complete. Scanning electron microscopy (SEM) characterization reveals that the polyurethane plugging system possesses a “sea-island” biphasic structure, forming a strong and ordered hydrogen bond network that provides higher strength and better thermal stability.

(3) Simulation-based evaluation of sealing performance indicates that the polyurethane sealing system exhibits high sealing efficiency and breakthrough pressure gradients. The 40%+2% polyurethane sealing system demonstrates superior curing performance compared to the 30%+2% system, achieving a maximum sealing efficiency of 96% and a maximum breakthrough pressure gradient of 4.2 $MPa \cdot m^{-1}$.

Funding

Supported by the Research Start-up Fund of the Karamay Campus, China University of Petroleum (Beijing) (No. XQZX20240013); the Natural Science Foundation of the Xinjiang Uygur Autonomous Region (2025D01A151); and the 2025 Karamay City Innovation Environment Development Program (Innovative Talent) (No. 2025DB0080)

About the Author

Qianbing Lin was born in 2005 in the Guangxi Zhuang Autonomous Region, China. She is currently pursuing her undergraduate degree at the Karamay Campus of China University of Petroleum (Beijing), where her primary research focus is oilfield chemistry.

Shiyu Wang was born in Shanxi in 2004. He is currently pursuing his undergraduate degree at the Karamay Campus of China University of Petroleum (Beijing), where his

research focuses on oilfield chemistry.

Lianghui Guo was born in Henan, China, in 1988. He is a full-time lecturer at the Karamay Campus of China University of Petroleum (Beijing). He graduated from China University of Petroleum (Beijing) in June 2023 with a Ph.D. in Oil and Gas Storage and Transportation Engineering. His primary research interests include oilfield chemistry and surface engineering.

References

[1] Liu, X., Wu, J., Hu, J., et al. (2025). Development of a polyurethane lost circulation material suitable for malignant leakage of drilling fluid. Processes, 13(11), 3707. doi: 10.3390/pr13113707.

[2] Huo, J., Zhang, H., Wei, C., et al. (2025). Oil-soluble temporary plugging agent used for drilling reservoir protection: Preparation, characteristics and mechanism. Journal of Applied Polymer Science, 142(42), e57611. doi: 10.1002/app.57611.

[3] Qin, L., Kou, D., Jiang, X., et al. (2025). Research progress on polyurethane-based grouting materials: Modification technologies, performance characterization, and engineering applications. Polymers, 17(17), 2313. doi: 10.3390/polym17172313.

[4] Wu, S., Ma, S., Zhang, Q., et al. (2025). A comprehensive review of polyurethane: Properties, applications and future perspectives. Polymer, 327, 128361. doi: 10.1016/j.polymer.2025.128361.

[5] Wang, L., Xiang, S., Ling, G., et al. (2025). New modification strategy for thermoplastic polyurethane with high hygrothermal ageing resistance and flame retardancy. Polymer Degradation and Stability, 232, 111140. doi: 10.1016/j.polymdegradstab.2024.111140.

[6] Choi, E. Y., & Kim, C. K. (2023). Degradation and lifetime prediction of thermoplastic polyurethane encapsulants in seawater for underwater acoustic sensor applications. Polymer Degradation and Stability, 209, 110281. doi: 10.1016/j.polymdegradstab.2023.110281.

[7] Tayefi, M., Eesaee, M., Hassanipour, M., et al. (2023). Recent progress in the accelerated aging and lifetime prediction of elastomers: A review. Polymer Degradation and Stability, 214, 110379. doi: 10.1016/j.polymdegradstab.2023.110379.

[8] Li, Y., Wu, J., Chen, Z., et al. (2024). The influence of oil and thermal aging on the sealing characteristics of NBR seals. Polymers, 16(17), 2501. doi: 10.3390/polym16172501.

[9] Li, H., Huang, X.-B., Sun, J.-S., et al. (2023). Improving the anti-collapse performance of water-based drilling fluids of Xinjiang Oilfield using hydrophobically modified silica nanoparticles with cationic surfactants. Petroleum Science, 20(3), 1768–1778. doi: 10.1016/j.petsci.2022.10.023.

[10] Liu, J., Fu, H., Luo, Z., et al. (2023). Preparation and performance of pH-temperature responsive low-damage gel temporary plugging agent. Colloids and Surfaces A: Physicochemical and Engineering Aspects, 662, 130990. doi: 10.1016/j.colsurfa.2023.

130990.

[11] Zou, C., Dai, C., Liu, Y., et al. (2023). A novel self-degradable gel (SDG) as liquid temporary plugging agent for high-temperature reservoirs. Journal of Molecular Liquids, 386, 122463. doi: 10.1016/j.molliq.2023.122463.

[12] Liu, C., Zou, H., Wang, Y., et al. (2024). Degradation behavior and mechanism of P(AM/AA/AMPS)@PLA core-shell self-degrading temporary plugging agent. Journal of Molecular Liquids, 393, 123656. doi: 10.1016/j.molliq.2023.123656.

[13] Xu, H., Zhang, L., Wang, J., et al. (2023). Evaluation of self-degradation and plugging performance of temperature-controlled degradable polymer temporary plugging agent. Polymers, 15(18), 3732. doi: 10.3390/polym15183732.

[14] Yang, F., Liu, J., Ji, R., et al. (2024). Degradable gel for temporary plugging in high temperature reservoir and its properties. Gels, 10(7), 445. doi: 10.3390/gels10070445.

[15] Niu, C., Fan, S., Chen, X., et al. (2024). Preparation and performance evaluation of a supramolecular polymer gel-based temporary plugging agent for heavy oil reservoir. Gels, 10(8), 536. doi: 10.3390/gels10080536.

[16] Yang, Z., Ni, R., Yang, Y., et al. (2024). Carboxymethyl cellulose-based supramolecular hydrogel with thermo-responsive gel-sol transition for temporary plugging of oil pipeline in hot work. Carbohydrate Polymers, 324, 121556. doi: 10.1016/j.carbpol.2023.121556.

[17] Dai, L., Sun, J., Lv, K., et al. (2025). Cellulose nanofiber-reinforced supramolecular polymer gels for temporary plugging of fractured oil and gas reservoirs. Carbohydrate Polymers, 356, 123370. doi: 10.1016/j.carbpol.2025.123370.

[18] Bai, Y., He, J., Sun, J., et al. (2024). Plugging performance and mechanism of an OBDF oil-absorbing resin (MMA-SMA-St) plugging agent. RSC Advances, 14, 21107–21117. doi: 10.1039/D4RA02420F.

[19] Dong, S., He, L., Li, L., et al. (2023). Investigation of polyvinyl alcohol–phenolic aldehyde–polyacrylamide gel for the application in saline oil reservoirs for profile modification. Energy & Fuels, 37(18), 13710–13720. doi: 10.1021/acs.energyfuels.3c02178.

[20] Chen, Y., Sang, Y., Guo, J., et al. (2023). Liquid–solid phase-change autogenous proppant fracturing fluid—Phase-change behavior research and field application. Energy & Fuels, 37(21), 16333–16344. doi: 10.1021/acs.energyfuels.3c01266.